J Electr Eng Technol Vol. 9, No. 3: 1072-1079, 2014
http://dx.doi.org/10.5370/JEET.2014.9.3.1072

ISSN(Print) 1975-0102
ISSN(Online) 2093-7423

Coordinated Droop Control for Stand-alone DC Micro-grid

Hyun-Jun Kim*, Yoon-Seok Lee*, Jae-Hyuk Kim* and Byung-Moon Han†

Abstract – This paper introduces a coordinated droop control for the stand-alone DC micro-grid, which is composed of photo-voltaic generator, wind power generator, engine generator, and battery storage with SOC (state of charge) management system. The operation of stand-alone DC micro-grid with the coordinated droop control was analyzed with computer simulation. Based on simulation results, a hardware simulator was built and tested to analyze the performance of proposed system. The developed simulation model and hardware simulator can be utilized to design the actual stand-alone DC micro-grid and to analyze its performance. The coordinated droop control can improve the reliability and efficiency of the stand-alone DC micro-grid

Keywords: Stand-alone DC micro-grid, Autonomous control, Droop control, PV (photo-voltaic) generator, WP (wind power) generator, BES (battery energy storage), SOC (state of charge), MPPT (maximum power point tracking)

1. Introduction

Stand-alone micro-grid is a small power grid without any connection with the utility AC grid. It is only composed of renewable power sources, engine generator, BES (battery energy storage), and load. Stand-alone micro-grid can be implemented with AC backbone network or DC backbone network.

Stand-alone AC micro-grid has inherent disadvantages related to synchronization, stability, and reactive power. However, stand-alone DC micro-grid does not have these disadvantages. It has relatively lower loss and cost due to the direct connection through one-stage power conversion. Stand-alone DC micro-grid can directly supply power to the digital loads, such as computers, communication devices, and automation devices, which consume DC power internally [1-3].

The control method for stand-alone DC micro-grid is divided into two groups. One is a real-time direct control according to the operation mode, in which the generated, stored, and consumed power are measured and transmitted to the main controller through high-speed communication link [4-6]. This method can offer highly safe operation for the micro-grid if a fast data transmission between the main controller and the local controllers is possible.

Another method is an autonomous control without communication link, in which the converter output voltage is regulated using droop control [7-10]. This method improves the performance degradation due to the circulating current among the connected converters. However, it brings about rather high transients and slow dynamic response in regulation process.

This paper introduces a coordinated droop control for stand-alone DC micro-grid, which can improve these weak points. The operation of stand-alone DC micro-grid with coordinated droop control was analyzed using simulation with PSCAD/EMTDC [11, 12]. Based on simulation results, a hardware simulator was built and tested to verify the performance of stand-alone DC micro-grid.

2. Stand-alone DC Micro-grid

Fig. 1 shows the configuration of stand-alone DC micro-grid, which is composed of uncontrollable power sources like a WP (wind power) generator and PV (photo-voltaic) generator, controllable power source like an engine generator and BES (battery energy storage), and load. It

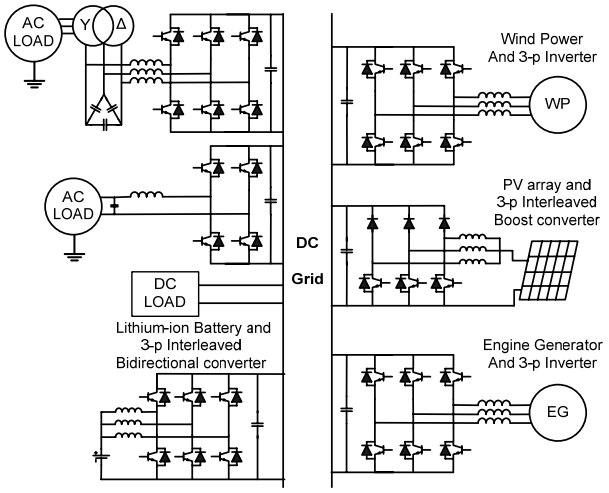

Fig. 1. System structure of stand-alone DC micro-grid

† Corresponding Author: Dept. of Electrical and Electronic Engineering, Myongji University, Korea. (erichan@mju.ac.kr)
* Dept. of Electrical and Electronic Engineering, Myongji University, Korea. (Inverter1112@naver.com)
Received: November 7, 2013; Accepted: March 7, 2014

also has a monitoring system to supervise whole system operation through communication link. Each converter has a local controller to manage the operation of each source, BES, and load.

WP generator has a 3-phase AC-DC converter to convert the 3-phase AC power into the DC power. Particularly, the AC-DC converter for WP generator includes a control scheme for MPPT (maximum power point tracking). PV generator has an interleaved DC-DC converter to convert the variable DC voltage into the regulated DC voltage.

It also has a control scheme for MPPT. BES has a bidirectional interleaved DC-DC converter to step down the DC grid voltage for charging or step up the battery voltage for discharging. Engine generator and AC load are connected to the DC grid through the DC-AC converter. And the DC load is connected to the DC grid directly or through another DC-DC converter.

3. System Operation and Control

3.1 Circulating current suppression

The stand-alone DC micro-grid described in this paper does not use communication link for control purpose, but it uses communication link for monitoring purpose in autonomous control. When the autonomous control is applied for power balancing, circulating current occurs at each converter due to sensor error, control error, and line voltage drop. The circulating current between each converter is directly related to the system loss. So, special scheme to suppress the circulating current is required.

The BES has a DC voltage control which is shown in Fig. 2. If error occurs in the voltage controller, circulating current flows. One scheme to suppress this circulating current is to insert a resistance between the DC grid and the converter. But this scheme is not practically reasonable in the point of loss, cost, and size.

In this paper a feedback loop was added to adjust the droop voltage, in which the DC current I_{BES_OUT} is measured and multiplied by the virtual resistance R_V to reduce the reference DC droop voltage.

$$V_{DROOP}^{*} = V_{Rate} - R_V \times I_{BES\_OUT} \quad (1)$$

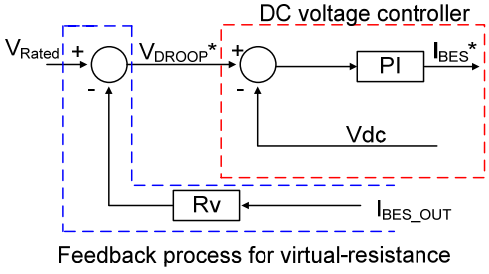

Fig. 2. Droop control for BES

Therefore, the reference DC voltage can be adjusted by this feedback loop without inserting resistance.

The virtual resistance can be derived considering the tolerable voltage variation as the following equation.

$$R_V = \frac{\Delta V_{dc} \times V_{\min}}{k \times P_{Rate}} \quad (2)$$

Where, the V_{min} is the minimum DC grid voltage and the P_{Rate} is the rated converter capacity.

3.2 Coordinated droop control

Fig. 3 shows an operation scheme for the proposed coordinated droop control method for the controller of BES. The droop curve is divided into three regions according to the DC grid voltage and the battery SOC. The slope of droop curve in region A and B are same and the slope of droop curve in region C is deferent from that of droop curve in region A and B. So, the virtual resistance is also different, which produces the reference value of droop voltage using Eq. (1).

Region A is located in the DC grid voltage with tolerance of +3 ~ +5% or -3% ~ -5%. In this region the battery operates at 100% rated power. The virtual resistance at this region is obtained from Eq. (3). At over +3% zone the engine generator reduces the output power to handle the surplus power in the DC grid. At under -3% zone the engine generator increases the output power to handle the deficient power in the DC grid.

Region B is located in the DC grid voltage with tolerance of -3~+3%. In this region the battery operates at 70% of rated power. The virtual resistance at this region is obtained from Eq. (3).

Region C is defined as a protection zone for over charge and over discharge. In this region, the converter reduces the charging or discharging power immediately to protect the battery. The handling power is about 10% rated power and the virtual resistance at this region is obtained from Eq. (4).

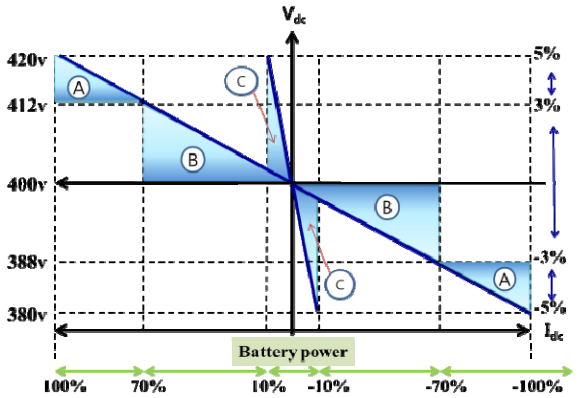

Fig. 3. Coordinated droop control for BES

$$\Delta V_{dc} = 20[V](5\%), V_{dc\_min} = 380[V]$$
$$P_{BES} = 5.0[kW], R_{BES} = \frac{\Delta V_{dc} \times V_{dc\_min}}{P_{BES}} = 1.52[\Omega] \quad (3)$$

$$\Delta V_{dc} = 20[V](5\%), V_{dc\_min} = 380[V]$$
$$P_{BES} = 1.0[kW], R_{BES} = \frac{\Delta V_{dc} \times V_{dc\_min}}{P_{BES}} = 7.6[\Omega] \quad (4)$$

3.3 EG operation scheme

The EG operation scheme is described in Fig. 4, in which the EG output power is autonomously controlled according to the voltage variation of DC grid. If the output power of PV and WP is smaller than the power demand in load, the BES discharges power to maintain the power balance in the DC grid.

If the discharged energy increases and the voltage variation decreases down lower than -3%, the EG output power is repeatedly raised by △P to maintain the voltage variation at -3%. When the grid voltage variation is larger than +3%, the EG output power is repeatedly decreased by △P to maintain the voltage variation at +3%. So, the EG output power is autonomously controlled for effective energy management without predicting the load pattern.

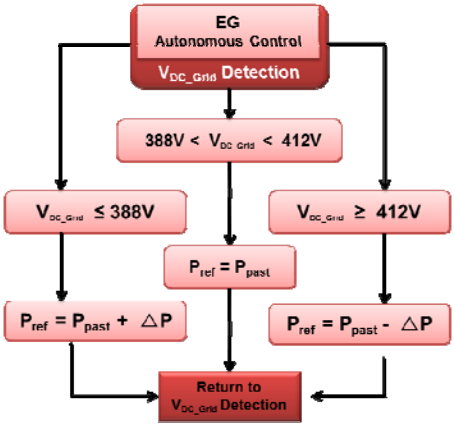

Fig. 4. Operation scheme for EG

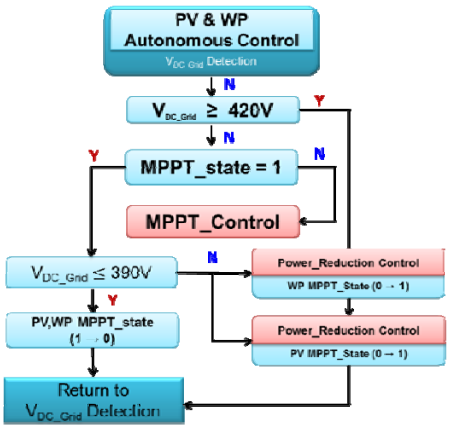

Fig. 5. Operation scheme for PV and WP

3.4 PV and WP operation scheme

Since the output power of PV or WP changes continuously according to the weather condition, PV or WP operates in MPPT mode. If the voltage variation of DC grid overreaches at +5%, it can brings about stability problem in the DC grid. And it overcharges the BES to make shortening the battery life.

Therefore, if the DC grid voltage is higher than 420V, the PV or WP output power is decreased to reduce the DC grid voltage separately or together. When the DC grid voltage is located under the rated voltage, it means power deficiency in the DC grid. In this case, the output power of PV or WP restart to operates in MPPT mode. So, the output power of PV and WP is autonomously controlled to make the power balance at the DC grid.

3.5 BES operation scheme

The operation sequence for BES is shown in Fig. 6. When the battery SOC is between 20% and 80%, power-balancing control is selected for droop control. Depending on the variation of DC grid voltage, region A, B, C are selected.

If the variation of DC grid voltage is less than -3% or larger than +3%, the droop control is carried out in region A. The output power of BES is set at 70%~100% of the rated power. If the variation of DC grid voltage is located between -3% and +3%, the droop control is carried out in region B. The output power of BES is set at 0%~70% of the rated power. The virtual resistance is determined by 1.52Ω.

When the battery SOC is larger than 80% or less than 20%, the DC grid voltage is checked whether it is higher than 400V or not. If higher, the droop control is carried out in region C. The output power of BES is at 10% of the rated power. If not, the charging mode is changed to the discharging mode or the discharging mode is changed to the charging mode. The virtual resistance is determined by 7.6Ω

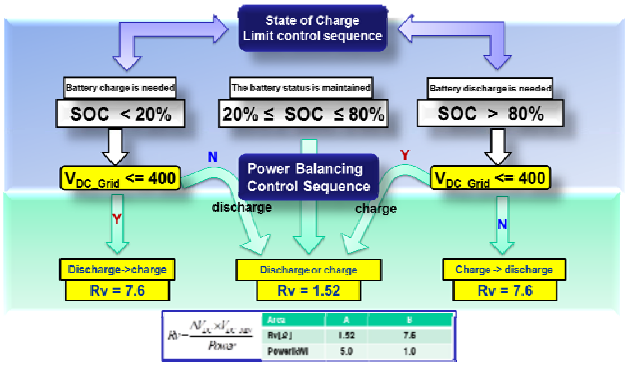

Fig. 6. Operation scheme for BES

4. Computer Simulation

Fig. 7 shows a structure of converter control in the stand-alone DC micro-grid. PV controller consists of current control to implement the MPPT, which is a nonlinear function of irradiation and temperature. WP controller also consists of current control to implement the MPPT, which is achieved by keeping the power coefficient of blade to have maximum value regardless of varying wind-speed. WP controller consists of outer speed control and inner current control. EG (engine generator) operates to adjust the output power according to the reference value.

EG controller also consists of outer speed control and inner current control. BES controller consists of current control and DC voltage control. Depending on the sign of current value, charging or discharging operation is carried out [13, 14]. Three kinds of load can be connected to the DC micro-grid, which are a DC load, 1-phase load, and 3-phase load.

For the purpose of verifying the coordinated droop control, various simulations were carried out using the PSCAD/EMTDC software. The power circuit and the PWM converter were modeled with the built-in model, where as the PV and WP generators with controllers are implemented with a user-defined model coded in C language.

In order to obtain realistic verification, the simulation models for PV and WP were developed using the built-in model and the user-defined model coded with C language. The voltage and current characteristics of PV were represented using the PV characteristic equation. And the voltage and current characteristics of WP were represented using wind turbine model and synchronous generator model.

The voltage and current characteristic of lithium polymer battery were represented using the battery characteristic equation, in which the SOC (state of charge) is represented using current integration method [10]. The battery capacity unit is normally represented by Ah (Ampere-hour).

However, As (Ampere-sec) was used in simulation because Ah is too large to represent the battery capacity in the simulation time of a few ten sec. Table 1 shows the simulation parameter of each component in the stand-alone DC micro-grid.

Simulation scenario and checking items were prepared to verify all the operation characteristics of stand-alone DC micro-grid. Table 2 shows all the checking items in each section of simulation time which indicates the operation regions in Fig. 3. Total simulation time is 20s and 11 time sections are divided to check the operation characteristic.

Fig. 8 shows the simulation results for the coordinated droop control. The 1st, 2nd, 3rd, 4th, 5th graphs show the load power, WP power, PV power, EG power, and BES power respectively. The 6th, 7th, 8th graphs show the DC

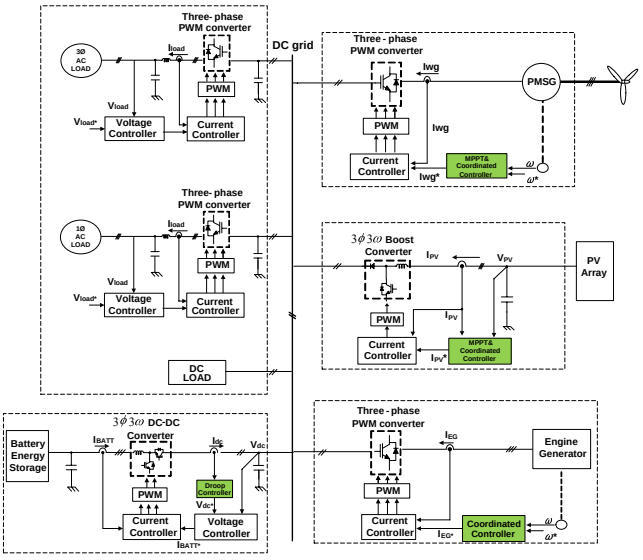

Fig. 7. Converter control for stand-alone DC micro-grid

Table 1. Simulation parameters of each component in stand-alone dc micro-grid.

Engine Generator	Rated Power	Rated Voltage	Rated Current	Rated Frequency	Rated Velocity
	5 [kW]	200 [V]	15 [A]	400 [Hz]	1714 [rpm]
Wind Power Generator	Rated Power	Rated Voltage	Rated Current	Rated Frequency	Rated Velocity
	5 [kW]	220 [V]	13 [A]	60 [Hz]	1800 [rpm]
PV Array	Rated Power	V_{MPPT}	I_{MPPT}	C_{PV}	L_{PV}
	5 [kW]	250 [V]	20 [A]	270 [uF]	2 [mH]
Lithium-Polymer Battery	Rated Power	Rated Voltage	Rated Current	L_{BAT}	Internal Resistance
	5 [kWh]	250 [V]	20 [Ah]	2 [mH]	0.0047 [ohm]
Load (3EA)	Rated Power	Rated Voltage	Rated Current	L_{LOAD}	C_{LOAD}
	3.3 [kW]	220 [V]	15 [A]	4 [mH]	10 [uF]

Table 2. Simulation scenario and checking items.

No.	Checking items in simulation	Region
1	EG coordinated control (Up to+70% of rated battery)	B
2	+100% of rated battery power	A
3	Distributed generation production	B
4	EG Coordinated Control (Up to -70% of rated battery)	B
5	-100% of rated battery power	A
6	PV coordinated control (output power reduction)	A
7	PV coordinated control (maximum output power)	A
8	Battery charging mode	B
9	Droop curve change (Soc >80%) & (R_V : 1.52Ω → 7.6Ω)	C
10	Wind coordinated control (output power reduction)	B
11	Wind coordinated control (maximum output power)	B

grid voltage, virtual resistance, and SOC. It is assumed that the load power changes from 0 to 10kW, and the PV and WP powers change from 0 to 5kW so that all the operation regions can be involved.

In section 1, both PV and WP power were set at 0kW and the load power slowly increased up to 8.5kW in order to make the droop control operates in region B. The BES primarily supplies the load power of 3.5kW with 70% portion and the remaining power from 3.5 to 8.5kW is supplied from the EG. Through these graphs the coordinated control of EG can be verified.

In section 2, the load power increased from 8.5 to 10kW and the operation region of droop control changed from B to A. Since the EG already supplies 5kW power to the load, more required power in load should be supplied from the BES. So, the BES changes the load sharing portion from 70% to 100%.

In section 3 and 4, both PV and WP power were increased from 0 to 5kW and the load power decreased from 10 to 6.5kW. The operation mode of BES changes from discharging to charging. The output power of EG is reduced from 5 to 0kW through coordinated control. The BES is protected from the over-discharge and the operation region changes from A to B.

In section 5, the PV and WP power is set at the rated power and the load power is reduced. So, even though the EG output power is reduced, the DC grid voltage rises due to the surplus power in the DC grid. Because of the surplus power in the DC grid, the sharing portion of BES is changed from 70% to 100%.

In section 6, the load power is decreased down to 2.5kw and increased up to 8kW. When the DC grid voltage reaches at 419V, the PV power is removed to suppress the rise of DC grid voltage.

In section 7, the load power is increased from 8 to 10kW and the DC grid voltage decreases due to the power deficiency. When the DC grid voltage reaches at 390V, the PV power is restarted and the operation region changes from A to B.

In section 8 and 9, the PV and WP power is larger than the load power and the BES is slowly charged. When the SOC of battery reaches at the maximum value of 80%, the virtual resistance Rv is changed from 1.52Ω to 7.6Ω. The operation region changes from B to C and the sharing portion of BES is changed from 70% to 10%. So, it is verified that the SOC limit is properly managed.

In section 10 and 11, the power balance can be maintained by reducing the PV, WP, EG powers and managing the SOC limit. AS the load power increases, the WP is restarted when the DC grid voltage reaches at 390V.

Using all the graphs shown in Fig. 8, the checking items described in Table 2 are verified. It is known that the coordinated droop control described in this paper works properly in three operation regions.

5. Integrated Operation Test

Based on simulation results, a hardware simulator for stand-alone DC micro-grid was built in the lab. Fig. 9

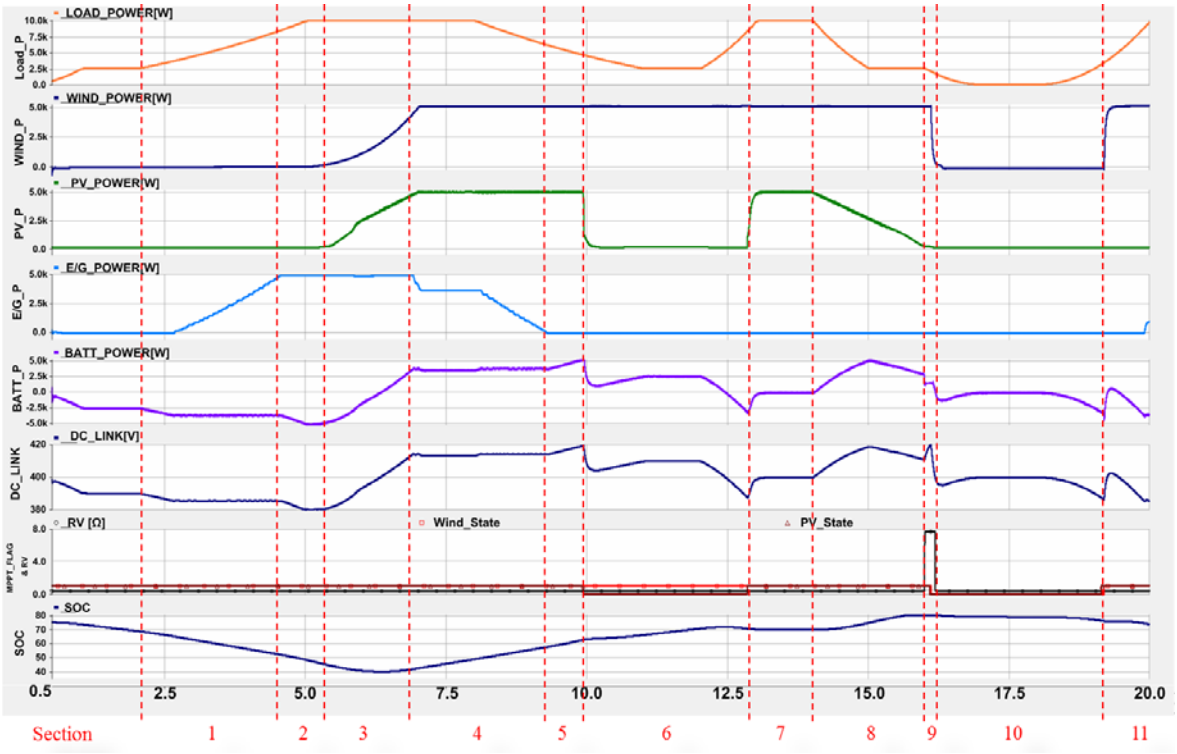

Fig. 8. Simulation results for stand-alone DC micro-grid

Fig. 9. Experimental set-up

shows experimental set-up of hardware simulator for integrated operation test. The hardware simulator consists of 5kW WP simulator, 5kW PV simulator, 5kW EG, 5kWh lithium-polymer battery stack with battery management system, DC micro-grid assembly, PC (personal computer) for main controller, and variable AC load.

The experimental data of integrated operation test are displayed on the 16-channel oscilloscope. Each converter sub-assembly is mounted on the small iron drawer. DC bus is installed on the back side of DC micro-grid assembly, in which all the output terminal of DGs, BES, and DC load are connected together.

The wind power simulator and the PV simulator can produce arbitrary output power according to the wind speed and the irradiation. The BES has a BMS (battery management system) which provides SOC data through CAN communication. A touch-screen monitor was mounted in front of the hardware so that all the output powers from the PV, WP, BES, Load and the operation state can be monitored. RS-485 communication link was used for data transmission and gathering.

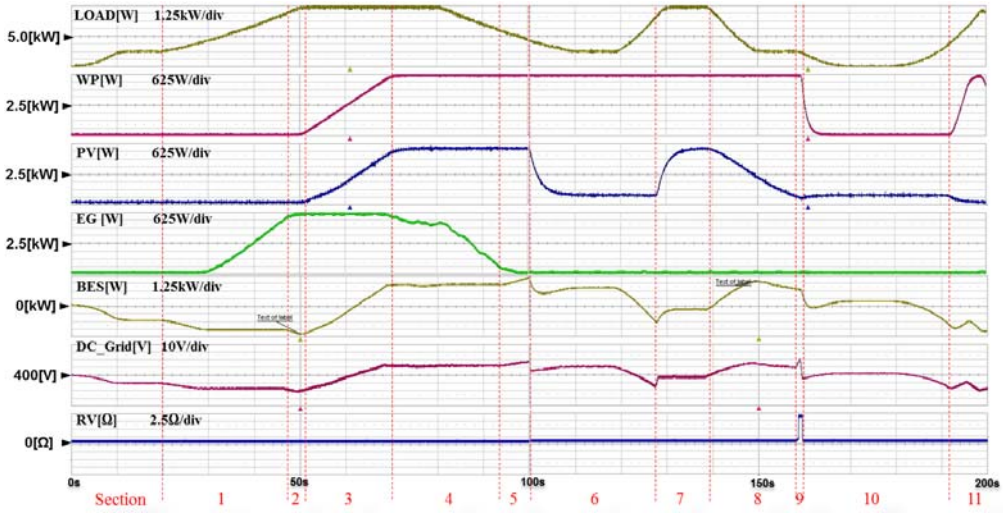

Fig. 10. Experimental set-up for integrated test

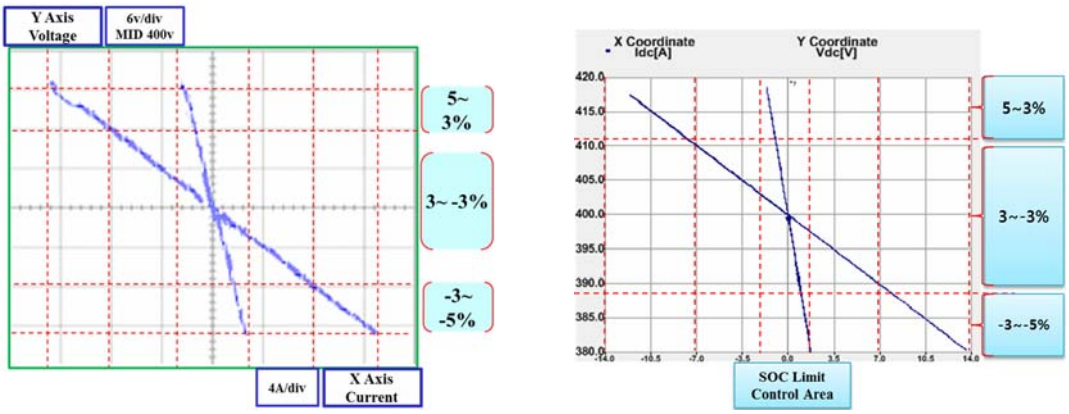

(a) (a)

Fig. 11. Coordinated droop and SOC limit curve

Fig. 10 shows the experimental results for the stand-alone DC micro-grid with applying the coordinated droop control. The basic assumptions for the experiment are exactly same as those for simulation. The only difference is the time scale for experiment. The maximum time scale used in the experiment is 200s, while the maximum time scale used in the simulation is 20s. All the measured graphs have almost identical shapes to those shown in the simulation. Using all the graphs shown in Fig. 11, the checking items described in Table 2 are verified experimentally. It is confirmed that the coordinated droop control described in this paper works properly in three operation regions.

Fig. 11(a) shows the measured droop curves for the voltage and current of DC micro-grid, while Fig. 11(b) shows the simulated droop curves for the voltage and current of DC micro-grid. Through these two figures it is confirmed that the coordinated droop control for the DC micro-grid operates properly as expected. Therefore, the coordinated droop control can offer very safe operation of DC micro-grid without high transients.

6. Conclusion

This paper introduces a new operation method with coordinated droop control for stand-alone DC micro-grid. The proposed coordinated droop control can offer improvement of system reliability and efficiency for the stand-alone DC micro-grid, which is composed of WP, PV, EG and BES with SOC (state of charge) management system. The operation of stand-alone DC micro-grid with proposed control was analyzed using simulation with PSCAD/EMTDC.

Based on simulation results, a hardware simulator was built and tested to analyze the performance of proposed system. The developed simulation model and hardware simulator can be utilized to design the actual stand-alone DC micro-grid and to analyze its performance with practical manner.

Acknowledgements

This work was supported by the Human Resources Development program (No. 20134030200310) and the research project (No. 20111020400080) of the Korea Institute of Energy Technology Evaluation and Planning (KETEP) grant funded by the Korea government Ministry of Trade, Industry and Energy.

References

[1] D. Salomonsson, L. Sode, A. Sannino, “An Adaptive Control System for a DC Microgrid for Data Centers”, IEEE Transactions on Industry Applications, Vol. 44, No. 6, pp. 1910-1917, Nov, 2008.

[2] H. Kakigano, Y. Miura, T. Ise, “Low-Voltage Bipolar-Type DC Microgrid for Super High Quality Distribution”, IEEE Transactions on Power Electronics, Vol. 25, No. 12, pp. 3066-3075, Dec, 2010.

[3] P. Biczel, “Power Electronic Converters in DC Microgrid”, IEEE CPE'07 (Compatibility in Power Electronics 2007), Gdynia, Poland, May 29-Jun 01, 2007.

[4] Bi. Rui, Ding. Ming, Xu. Ting Ting, “Design of common communication platform of microgrid”, IEEE Power Electronics for Distributed Generation Systems (PEDG), June 16-18, 2010.

[5] A. Ruiz-Alvarez, A. Colet-Subirachs, O. Gomis-Bellmunt, J.M. Fernàndez -Mola, J. López-Mestre, A. Sudria -Andreu, “Design, management and comissioning of a utility connected microgrid based on IEC 61850”, Innovative Smart Grid Technologies Conference Europe (ISGT Europe), Oct 11-13, 2010.

[6] Byong-Kwan Yoo, Seung-Ho Yang, Hyo-Sik Yang, Won-Yong Kim, Yu-Seok Jeong, Byung-Moon Han, Kwang-Soo Jang, “Communication Architecture of the IEC 61850-based Micro Grid System", Journal of Power Electronics, vol. 11, no. 3, pp. 350-359, May, 2011.

[7] F. Katiraei, R. Iravani, P. Lehn, “Micro-grid autonom ous operation during and subsequent to islanding process” IEEE Transaction on Power Delivery, Vol. 20, No. 1, pp. 248-257, Jan, 2005.

[8] P. Piagi, R.H. Lasseter, “Autonomous control of microgrids”, IEEE PESGM (Power Engineering Society General Meeting), Oct, 2006.

[9] C. Lee, C. Chu, P. Cheng, “A New Droop Control Method for the Autonomous Operation of Distributed Energy Resource Interface Converters”, IEEE Transactions on Power Electronics, Vol. 28, No. 4, pp. 1980-1993, 2013.

[10] B. Meersman, J.D.M. De Kooning, L. Vandevelde, “Analogy Between Conventional Grid Control and Islanded Microgrid Control Based on a Global DC-Link Voltage Droop”, IEEE Transactions on Power Delivery, Vol. 27, No. 3, pp. 1405-1414, July, 2012.

[11] Il-Yop Chung, Wenxin Liu, David A. Cartes, Soo-Hwan Cho and Hyun-Koo Kang, “Controller Optimization for Bidirectional Power Flow in Medium-Voltage DC Power Systems”, JEET, vol. 6, no. 6, pp. 750-759, 2011

[12] Ji-Heon Lee, Hyun-Jun Kim, Byung-Moon Han, Yu-Seok Jeong, Hyo-Sick Yang and Han-Ju Cha, “DC Micro-grid Operational Analysis with a Detailed Simulation Model for Distributed Generations”, Journal of Power Electronics, vol. 11, no. 3, pp. 350-359, May, 2011.

[13] Jong-Yul Kim, Seul-Ki Kim, June-Ho Park, “Con-

tribution of an Energy Storage System for Stabilizing a Microgrid during Islanded Operation", JEET, vol. 7, no. 6, pp. 824-833, 2012

[14] Jong-Yul Kim, Seul-Ki Kim, June-Ho Park, "Coordinated State-of-Charge Control Strategy for Microgrid during Islanded Operation", JEET, vol. 4, no. 2, pp. 194-200, 2009

Hyun-Jun Kim He received his B.S. and M.S. degree in Electrical Engineering from Myongji University, Seoul, Korea, in 2011 and 2013, respectively. Currently, He is pursuing his Ph.D. degree in Myongji University. His research interests include power electronics applications for distributed generation and AC/DC micro-grid operation and control.

Yoon-Seok Lee He received his B.S. and M.S. degree in Electrical Engineering from Myongji University, Seoul, Korea, in 2012 and 2014, respectively. Currently, He is pursuing his Ph.D. degree in Myongji University. His research interests include power electronics applications for distributed generation and micro-grids.

Jae-Hyuk Kim He received his B.S. degree in Electrical Engineering from Myongji University, Seoul, Korea, in 2013. Currently, He is pursuing his M.S. degree in Myongji University. His research interests include Bidirectional Intelligent Semicon-ductor Transformer for Smart Grid

Byung-Moon Han He received his B.S. degree in Electrical Engineering from Seoul National University, Seoul, Korea, in 1976, and his M.S. and Ph.D. degrees from Arizona State University, USA, in 1988 and 1992, respectively. He was with the Westinghouse Electric Corporation as a Senior Research Engineer in the Science and Technology Center, Pittsburg, PA, USA. He is currently a Professor in the Department of Electrical Engineering, Myongji University, Seoul, Korea. His current research interests include power electronics applications for FACTS, custom power, distributed generation, and microgrid.